







## Extracting lamina parameters from response of laminates for inverse design of deployable structures

Ruiwen Guo , Ning An <sup>†,§,||</sup>, Xiaowei Yue , Xiaofei Ma <sup>‡</sup>,  
Qilong Jia <sup>†</sup> and Jinxiong Zhou <sup>†,\*¶,||</sup>

*\*State Key Laboratory for Strength and Vibration of  
Mechanical Structures and School of Aerospace,  
Xi'an Jiaotong University, Xi'an 710049, China*

*†Key Laboratory of Advanced Spatial Mechanism and Intelligent Spacecraft,  
Ministry of Education, School of Aeronautics and Astronautics,  
Sichuan University, Chengdu 610065, China*

*‡Xi'an Institute of Space Radio Technology,  
Xi'an 710100, China  
§anning@scu.edu.cn*

*¶jxzhouxx@mail.xjtu.edu.cn*

Received 8 April 2024

Revised 23 May 2024

Accepted 28 May 2024

Published 27 July 2024

Composite Tape-Spring Hinge (CTSH) is one of the basic components of space deployable structures achieving large-scale deployable mechanisms for various space missions. It is crucial to obtain the lamina parameters of the composite at the design stage to ensure that the CTSH possesses the required structural response. This work presents a strategy for extracting lamina parameters from structural response of CTSH based on optimization method. An efficient Artificial Neural Network (ANN)-based surrogate model is integrated into the optimization loop to replace the time-costing finite element simulation and establish the relationship between lamina parameters and bending response of CTSH. The inverse characterization process is achieved by minimizing the objective function defined as the error between the predefined target and output results from ANN model. The efficiency of the proposed strategy was validated by using a predefined bending moment-angle curve of CTSH with known lamina parameters, and an arbitrary bending moment-angle curve was inversely constructed to further demonstrate the capability in inverse design. It is shown that the proposed method can be applied not only to extract lamina parameters from structural response, but also to guide the selection of composite lamina based on the expected structural response of deployable structures.

*Keywords:* Space deployable structures; composite tape-spring hinge; surrogate models; inverse design; optimization.

PACS No.: 81.05.Qk

<sup>||</sup>Corresponding authors.

## 1. Introduction

As one of the basic components of space deployable structures,<sup>1,2</sup> the hinge performs the essential functions of connection, support, and state change between folded and deployed. Composite Tape-Spring Hinge (CTSH) is assembled from a single piece or multiple pieces of composite tape-springs, which can be folded elastically before and during launch to reduce storage volume and are able to self-deploy by releasing the stored strain energy.<sup>3,4</sup> Compared with mechanical hinges, the CTSH features the advantages of high strength/stiffness to weight ratio, low cost and ease of manufacture,<sup>5</sup> showing the potential for the application in space deployable structures. One of the most famous space missions is the MARSIS antenna onboard the Mars Express Spacecraft,<sup>6</sup> which contains three booms with several straight segments connected by CTSH. The RIME antenna in the recently launched JUICE spacecraft used the similar antennas connected by CTSH.<sup>7</sup> The application of CTSH in space missions leads to an in-depth investigation of CTSH over the past two decades. Mallikarachchi and Pellegrino<sup>4,5</sup> investigated the quasi-static folding and dynamic deployment behavior of CTSH through experiments and numerical simulations. Bai *et al.*<sup>8</sup> presented a shape optimization work of CTSH with the objectives of minimizing the mass and peak folding moment and maximizing the peak torsional moment. Jin *et al.*<sup>9</sup> formulated a multi-objective shape optimization problem of the CTSH to concurrently maximize the strain energy stored during the folding process and the peak bending moment during deployment.

The determination of the lamina parameters of composites is essential in the design of CTSH which directly controls its structural response. Each unidirectional lamina is considered as a transversely isotropic material, which contains five independent material parameters,  $E_1$ ,  $E_2$ ,  $\nu_{12}$ ,  $G_{12}$ ,  $G_{23}$ . The conventional approach to measuring these parameters includes manufacturing a group of specimens for each parameter and conducting a series of mechanical tests. However, factors, such as storage time and temperature variations,<sup>10,11</sup> and inherent experimental test data variations,<sup>12-15</sup> can significantly influence the measurement of these parameters, making accurately determination of all lamina parameters a time-consuming process with high cost. Moreover, the characterization of the material properties may lack precision in product analysis due to the manufacturing scattering in composite materials. Therefore, it is highly desirable to develop an inverse identification approach of lamina parameters from structural response.

The identification of lamina properties can be achieved by performing an indirect mechanical test on the laminated structures using an inverse approach. The lamina parameters are set as design variables and the objective function includes the residuals between experimental and numerical calculated structural response of laminated specimens. Then the identification process can be tackled by solving an optimization problem.<sup>16-19</sup> Based on optimization algorithm, iteratively updating the lamina parameters so that the output from the numerical model gets closer to the experimental one and finally the identification process is achieved by the

optimization. Soares *et al.*<sup>20–22</sup> successfully obtained the elastic properties of steel, aluminium and composite lamina from eigenfrequencies of plate specimens using a gradient-based optimization technique. Yu *et al.*<sup>23,24</sup> proposed an Abaqus-DNN framework to identify the constitutive parameters of composite materials from their response. The method is applicable to identify both stiffness properties and failure parameters of unidirectional composites. However, the iteration of the neural network depends on the gradient of output to input, which limits the potential of the method. On the other hand, genetic algorithm is more suitable and robust for solving the optimization problems involved with highly-nonlinear finite element calculations.<sup>25,26</sup> For example, Comellas *et al.*<sup>27</sup> identified the elastic and damage parameters from nonlinear force-displacement response of composite specimen with holes based on genetic algorithm.

It is known that genetic algorithm usually requires a significant amount of iterations and operations to converge to an optimal solution, especially when the design search space is high-dimensional. Therefore, surrogate model accelerated optimization method has been proposed and the effectiveness and accuracy have been well proven.<sup>28,29</sup> The surrogate model serves as a substitute for computationally intensive finite element simulations within the optimization loop. It provides the mapping relationship between lamina parameters and structural responses, enabling efficient exploration of the design space. A wide variety of well-established surrogate models have been used in inverse identification. Barkanov *et al.*<sup>30</sup> performed an inverse approach to characterize the viscoelastic properties from vibration test response with the aid of response surface model, which considerably decrease the computational efforts. Steuben *et al.*<sup>31</sup> used NonUniform Rational B-Spline (NURBS)-based surrogate to identify the parameters of isotropic-elastic, orthotropic-elastic and orthotropic-hyperelastic material from strain tensor components on the surface of the specimen. The Machine Learning (ML)-based Artificial Neural Network (ANN) model has strong fitting ability to give complex mapping relationships as a universal approximation,<sup>32,33</sup> which could be a better choice for constructing surrogate models. Jin *et al.*<sup>9</sup> trained an ANN-based surrogate model to correlate the cut-out shape parameters of CTSH with both the peak moment and the stored strain energy of the CTSH during the folding process. This surrogate model was then used to replace the finite element simulation to accelerate the iteration process to solve a shape optimization problem. Liu *et al.*<sup>34</sup> combined the ANN accelerated surrogate modeling and optimization algorithm to minimize the weight of laminated composite structures subject to a buckling constraint. The effectiveness and efficiency of the method were verified. Cappelli *et al.*<sup>35</sup> established an ANN surrogate model with pre-collected data to inversely characterize the uncertainty of elastic properties of the fiber and the matrix from first buckling load.

The main novelty of this work is to provide a surrogate model-accelerated optimization method for identification and inverse design of lamina parameters from structural response of CTSH. The structure of the CTSH is more complex than plate specimen and the folding response of CTSH is highly-nonlinear with complex

buckling and post-buckling characteristics. First, a parametric numerical simulation was conducted to collect the bending moment-angle curves of CTSH during folding process with different lamina parameters. The ANN surrogate model was then trained by the collected data to correlate the relation between the lamina parameters and response of CTSH. Finally, the objective function was constructed as the error between predicted and predefined target bending moment-angle curve and the surrogate model was imported into a genetic algorithm-based optimizer. The inverse identification was achieved by minimizing the objective function and the optimal result was the identified lamina parameters. The successful implementation of this process enables the inverse design of the CTSH with any desired bending moment-angle response and can be flexibly generalized to other composite deployable structures.

This paper is organized as follows. Section 2 describes FEM of the CTSH as well as the inverse identification strategy with the emphasis paid on the construction of the optimization problem. Two examples are chosen to validate the proposed approach and the identification results are presented in Sec. 3. Finally, discussions and conclusions are given in Sec. 4.

## 2. Methodology

The CTSH is made by cutting two opposite parallel slots on the composite thin-walled tube, each slot consists of a rectangle and two semicircles. Figure 1(a) illustrates the geometry of the CTSH considered in this work with dimensions labeled. As shown in Fig. 1(b), the composite thin-walled tube was manufactured using composite laminates consisting of two layers of unidirectional carbon fiber/epoxy lamina arranged in a stacking sequence of  $[+45^\circ, -45^\circ]$ . Each lamina (shown in

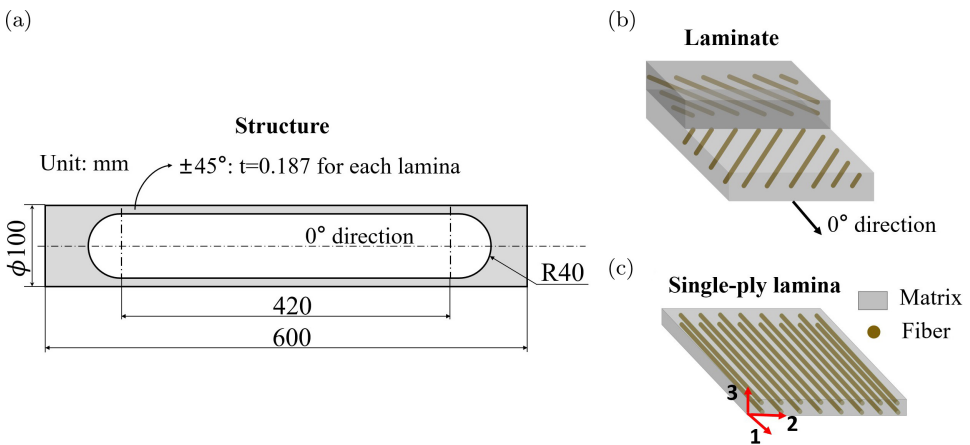


Fig. 1. (Color online) Modeling of CTSH. (a) Geometry of CTSH with dimensions. (b) Schematic of composite laminate, which consists of two layers of lamina arranged in a stacking sequence of  $[+45^\circ, -45^\circ]$ . (c) Schematic of single-ply composite lamina.

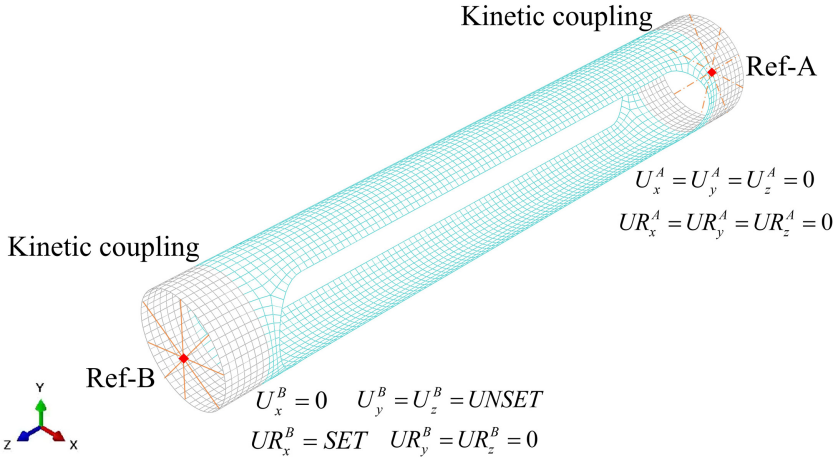


Fig. 2. (Color online) Finite element model of CTSH with boundary conditions and loads.

Fig. 1(c)) is considered a linear elastic and transversely isotropic material, described by five independent lamina parameters: Including the longitudinal elastic modulus  $E_1$ , transverse elastic modulus  $E_2$ , major Poisson's ratio  $\nu_{12}$ , in-plane shear modulus  $G_{12}$ , and out-of-plane shear modulus  $G_{23}$ , in which the subscript 1 represents the longitudinal direction of the fiber, while 2 and 3 represent the transverse directions perpendicular to the fiber. In addition, each lamina has a thickness 0.187 mm and a density 1.58 g/cm<sup>3</sup>.

Finite Element Model (FEM) simulations were performed to characterize the quasi-static folding process of the considered CTSH using a commercial finite element code Abaqus/Explicit 2020. A 3D FEM was constructed using shell element S4R with a global element size of 6 mm, as depicted in Fig. 2. The reference points A and B were coupled to the right and left ends of CTSH, respectively, by the kinematic coupling algorithm. The reference point A is fully fixed and the folding process of CTSH was achieved by applying a 180° rotation angle around the  $x$ -axis on reference point B in 3 s. Then the bending moment-angle curve during folding process is calculated.

The nominal lamina parameters of each layer were set as  $E_1 = 150.93$  GPa,  $E_2 = 9.99$  Gpa,  $\nu_{12} = 0.24$ ,  $G_{12} = 4.58$  GPa,  $G_{13} = 3.58$  GPa as an example. Figure 3(a) demonstrates the energy histories during the folding simulation of CTSH to ensure the quasi-static process and the structural response of CTSH was presented by bending moment-angle curve, as shown in Fig. 3(b). The most striking feature of the moment-angle curve is that the moment rose to a high peak and then remained almost constant until completely folded. We note that the accuracy of the FEM analysis has been validated against experimental tests in previous research.<sup>4,36</sup> Moment data between folding angles of 0.18° to 1.44° (31 data points in total) were chosen as the focus of our study because of its distinguishing features as shown in the orange area in Fig. 3(b).

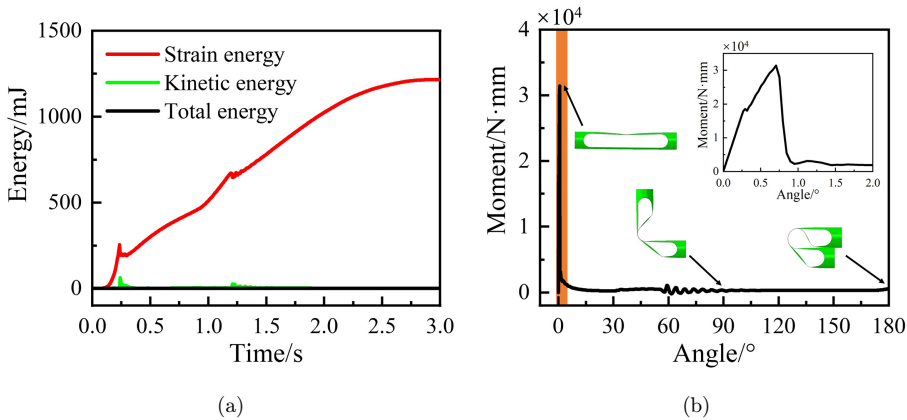


Fig. 3. (Color online) Simulation results of the folding process. (a) Variation of strain energy of CTSH during the quasi-static folding process. (b) Bending moment as a function of the rotational angle.

The forward solving process of obtaining the structural response with previously known lamina parameters has been intensively studied. The structural response such as the bending moment of CTSH is more convenient to measure experimentally than the lamina parameters of composite. In most cases, the required response of CTSH is determined first, followed by a selection for materials that fulfill the expectation. So, there exists a demand to identify lamina parameters from the response of the structure, which is an inverse approach. In this study, we adopted our previously proposed surrogate accelerated optimization framework<sup>9</sup> to solve the inverse problem. The work flow chart of this strategy is shown in Fig. 4, which is realized through a combination of design of experiment, parameterization of the CTSH, FEM simulation, surrogate modeling, and genetic algorithm-based optimization. This strategy can be further utilized for the inverse design of composite lamina that enables the structure to provide a specific response.

The first step is design of experiment, in which the lamina parameters were sampled to create the design space and the ranges of each lamina parameter are listed in Table 1. In order to ensure uniformly sample the five design variables, Latin hypercube technique was adopted and a total of 1000 sets of sampling data has been collected. Second, high-fidelity FEM simulations were performed for gathering data for the surrogate model training and testing. The commercial FEM code ABAQUS was used to calculate the bending moment of CTSH during folding process. The model as well as boundary condition have been described in Fig. 2. Python scripts were developed to drive the simulation process run automatically for each sampling point in design space and extract the response such as bending moment data. The third step uses the FEM database to build a surrogate model, there are several well-established surrogate modeling techniques available and the ML-based ANN model was chosen for our work. After trial-and-error, the structure of the ANN model was set as [5, 64, 31], meaning that the neural network has five inputs corresponding to

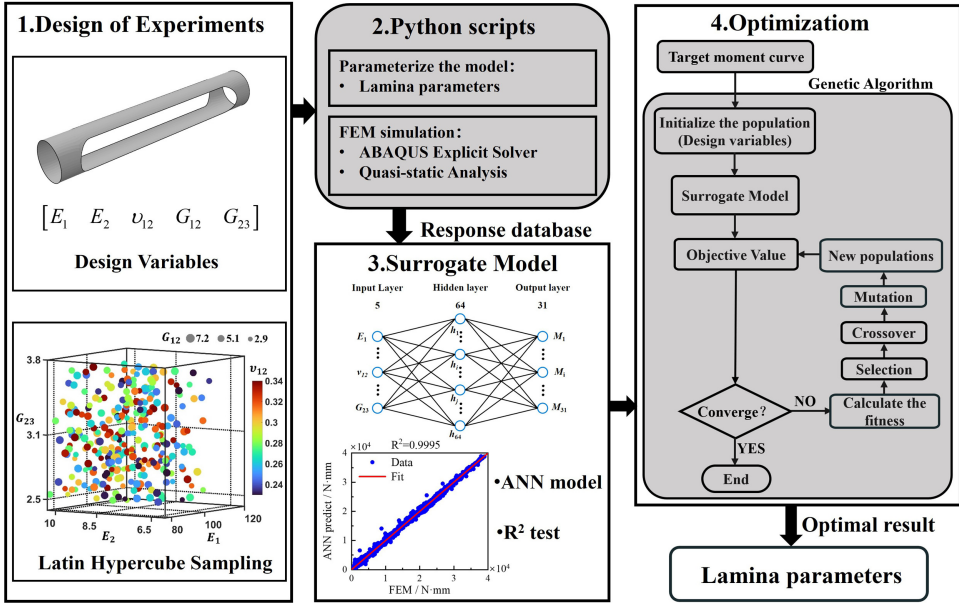


Fig. 4. (Color online) Work flow chart of the numerical strategy of minimize the error of bending moment-angle curve for extracting the corresponding material properties, which is realized through integration of design of experiment, parameterization of the CTSH, FEM simulation, surrogate modeling and genetic algorithm-based optimization.

five lamina parameters, 31 output representing 31 moment data points and one hidden layer with 64 neurons. The activation function was the Sigmoid function and the training algorithm was the Levenberg–Marquardt method. A comparison was made between FEM simulations and ANN predictions with a correlation coefficient of 0.9995 as shown in Fig. 5, the validity of the ANN surrogate model was verified. The ANN model gives an accurate mapping relationship between lamina parameters and structural response therefore the time-costing FEM simulations can be replaced by the ANN-based surrogate model. Finally, an optimization problem was proposed to inversely identify the lamina parameters. The solution of optimization problem was solved by genetic algorithm in MATLAB and accelerated with the aid of ANN surrogate model.

Specifically, the inverse approach we intend to achieve can be transformed into an optimization problem with an appropriately constructed objective function. The objective function was defined as the error between predefined and ANN predicted

Table 1. Upper limit and lower limit of unidirectional lamina parameters.

Parameters	$E_1$ [GPa]	$E_2$ [GPa]	$\nu_{12}$	$G_{12}$ [GPa]	$G_{23}$ [GPa]
Upper limit	181.00	10.30	0.34	7.17	3.71
Lower limit	80.00	6.67	0.23	2.93	2.50



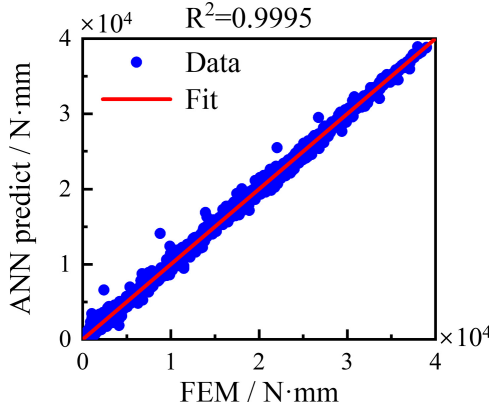


Fig. 5. (Color online) Performance of the surrogate model: correlation of ANN prediction versus FEM simulation, giving  $R^2$  up to 0.9995.

bending moment of CTSH during folding process which was expressed as follows:

$$E_r = \sqrt{\frac{\sum_{i=1}^n a_i (M_{\text{target},i} - M_{\text{predict},i})^2}{n}}, \quad (1)$$

where  $M_{\text{target},i}$  and  $M_{\text{predict},i}$  are the predefined target moment value and ANN surrogate model output moment value at the  $i$ th point, respectively. The total number of moment data points is  $n = 31$  and  $a_i$  are the weights of errors which are set as 0.1, 1, 0.01 for moment points  $i = 1-8$ ,  $i = 9-20$ ,  $i = 21-31$ , respectively, meaning that the data points close to the peak moment contribute more to the error.

The mathematical description of the optimization problem is now formulated as Eq. (2). The optimization variables are the five lamina parameters and were subjected to the same range of sample in the first step. By changing the optimization variables to minimize the value of objective function  $E_r$ , so that the moment curve of ANN output matches the predefined target one. Simultaneously, identification of lamina parameters was realized by the optimal results. The optimization problem was solved by genetic algorithm with the size of population set as 2000 and maximum number of iterations before the algorithm halts set as 800.

$$\begin{cases} \text{Find: } E_1, E_2, \nu_{12}, G_{12}, G_{23}, \\ \text{Minimize: } E_r, \\ \text{Subject to: } E_1 \in [80.00, 181.00], \quad E_2 \in [6.67, 10.30], \quad \nu_{12} \in [0.23, 0.34], \\ \quad \quad \quad G_{12} \in [2.93, 7.17], \quad G_{23} \in [2.50, 3.71]. \end{cases} \quad (2)$$

### 3. Results

A bending moment-angle curve of CTSH during the folding process with known lamina parameters was chosen as the target first to verify the efficiency of this



Table 2. Comparison of composite lamina parameters.

Parameters	Reference	Identified	Error
$E_1$ [GPa]	158.787	159.188	0.253%
$E_2$ [GPa]	7.636	7.595	0.537%
$\nu_{12}$	0.299	0.294	1.672%
$G_{12}$ [GPa]	5.294	5.292	0.038%
$G_{23}$ [GPa]	2.839	3.380	19.056%

method. The lamina parameters are listed in Table 2 as reference and the high-fidelity FEM simulation was performed in advance to obtain the target curve as the black line shown in Fig. 6(a). The convergence history during the genetic algorithm-based optimization can be seen in Fig. 6(b), which can be seen that the objective function of the best individual of each iteration decreases fast with the increase of iterations and finally reached an minimum value of 26.9 within 72 iterations. The optimal solution is a set of lamina parameters listed in Table 2, which is also the result of inverse identification approach from a target structural response. The lamina parameters identified are compared with the reference value, the error from reference is less than 2% for  $E_1$ ,  $E_2$ ,  $\nu_{12}$  and  $G_{12}$ , demonstrating the powerful identification capabilities of this strategy. However, the error of  $G_{23}$  from the reference value is slightly larger, close to 20%. This may be due to the  $G_{23}$  has sufficiently lower influence on the bending moment response of CTSH than other elastic characteristics and causes the identification difficulties. Figure 6(a) also compares the bending moment-angle curve calculated using the identified lamina parameters with the target one. The two curves coincide exactly, which further proves the correctness of this strategy.

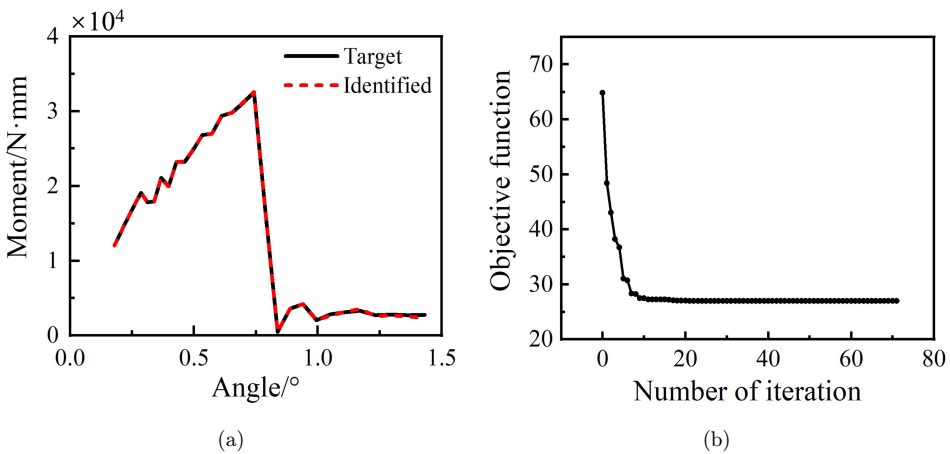


Fig. 6. (Color online) Identification result for a target moment-angle curve with pre-known lamina parameters. (a) Comparison of moment curve calculated using the identified lamina parameters and target curve. (b) Convergence history of the optimization process.

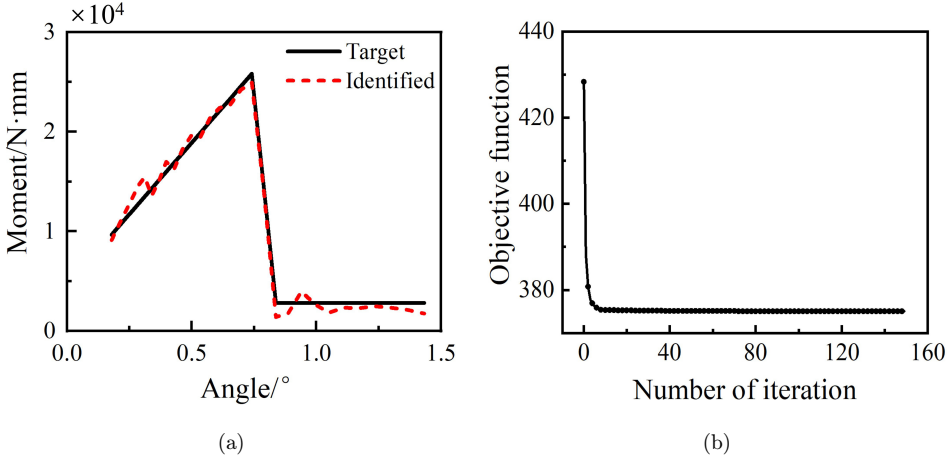


Fig. 7. (Color online) Identification result for an artificial moment-angle curve. (a) Comparison of moment curve calculated using the identified lamina parameters and target curve. (b) Convergence history of the optimization process.

Table 3. Lamina parameters identified with an artificial moment-angle curve as target.

Parameters	$E_1$ [GPa]	$E_2$ [GPa]	$\nu_{12}$	$G_{12}$ [GPa]	$G_{23}$ [GPa]
Identified	120.69	6.82	0.288	4.01	2.50

Furthermore, an arbitrary artificial bending moment-angle curve of CTS is constructed as the black line shown in Fig. 7(a), which consists of three straight lines without any knowledge of the related lamina parameters. Then the artificial curve was treated as the target for the optimization process with the convergence history was shown in Fig. 7(b). The objective function of the best individual reached an optimal value of 375.03 within 149 iterations and identified lamina parameters are listed in Table 3. The FEM simulation was then performed using the identified lamina parameters, and a comparison of the numerically calculated moment-angle curve and predefined artificial curve is shown in Fig. 7(a). The bending moment-angle curve calculated using the identified lamina parameters successfully captures all the features of artificial one, indicating that this strategy can be utilized to inverse design composite lamina parameters base on any expected structural response.

#### 4. Discussion and Conclusion

As a typical space deployable structure, the structural response of CTS during its folding and deployment process is crucial for its applications. The folding response of CTS is highly-nonlinear and involves complex buckling and post-buckling characteristics. Parameters of the composite lamina that constitutes the CTS


significantly affect the folding moment responses. However, the conventional approach to measuring these parameters is time-costing and inevitably there is usually some scatter in the experimental test data. In addition, structural analysis may not be accurate even with characterized material properties due to manufacturing errors. So, it is critical to accurately extract the corresponding lamina parameters from the structural response of CTSH.


To tackle the above-mentioned challenges, this work presents a strategy for inverse parametric identification of composite lamina from the structural response of CTSH. The identification process is transformed into an optimization problem in which the lamina parameters are set as design variables. The objective function is defined as the error between the numerically predicted and target bending moment-angle curve of CTSH. The ANN-based surrogate model is imported into the optimization loop to replace the time-costing FEM simulation and accelerate the process. By minimizing the objective function, the corresponding lamina parameters can be inversely extracted from an arbitrary bending moment-angle curve of CTSH. This strategy is feasible to inversely design the CTSH in terms of composite lamina selection depending on any desired structural response. It is worth mentioning that although our efforts are focused on the CTSH, the inverse parameter identification strategy proposed here, which integrates a forward-predictive surrogate model with optimization algorithms, is readily applicable to the investigation of other composite space deployable structures such as Composite Thin-Walled Lenticular Tube (CTLT) and Storable Tubular Extendible Members (STEM).


## Acknowledgments


This research was co-supported by the National Natural Science Foundation of China (Grants Nos. 11972277 and 12202295), the Fundamental Research Funds for the Central Universities (Nos. YJ2021137 and xzy022024052). Dr. Jia thanks the support by the Opening Project of Key Laboratory of Advanced Spatial Mechanism and Intelligent Spacecraft, Ministry of Education (Sichuan University).


## ORCID


Ruiwen Guo  <https://orcid.org/0009-0005-4720-0282>

Ning An  <https://orcid.org/0000-0002-4903-1559>

Xiaowei Yue  <https://orcid.org/0000-0002-5168-4014>

Xiaofei Ma  <https://orcid.org/0000-0002-8266-2539>

Qilong Jia  <https://orcid.org/0000-0002-6317-2008>

Jinxiong Zhou  <https://orcid.org/0000-0001-8453-7443>

## References

1. Z.-Q. Liu, H. Qiu, X. Li and S.-L. Yang, *Chin. J. Mech. Eng.* **30**(6) (2017) 1447.
2. N. An, M. Li and J. Zhou, *Int. J. Mech. Sci.* **180** (2020) 105753.

3. H. Mallikarachchi and S. Pellegrino, *J. Spacecraft Rockets* **51**(6) (2014) 1811.
4. H. Mallikarachchi and S. Pellegrino, *J. Spacecraft Rockets* **48**(1) (2011) 187.
5. H. Mallikarachchi and S. Pellegrino, *J. Spacecraft Rockets* **51**(2) (2014) 604.
6. M. Mobrem and D. S. Adams, *J. Spacecraft Rockets* **46**(2) (2009) 394.
7. E. Ecale, F. Torelli and I. Tanco, Juice interplanetary operations design: Drivers and challenges, in *SpaceOps Conf.* (Marseille, France, 2018), p. 2493.
8. T.-W. Liu, J.-B. Bai, N. Fantuzzi, G.-Y. Bu and D. Li, *Compos. Struct.* **280** (2022) 114757.
9. H. Jin, Q. Jia, N. An, G. Zhao, X. Ma and J. Zhou, *AIAA J.* **60**(10) (2022) 5942.
10. L. Musanje and B. Darvell, *Dental Mater.* **20**(8) (2004) 750.
11. R. A. Hawileh, A. Abu-Obeidah, J. A. Abdalla and A. Al-Tamimi, *Constr. Build. Mater.* **75** (2015) 342.
12. C. M. Hadden, D. R. Klimek-McDonald, E. J. Pineda, J. A. King, A. M. Reichenadter, I. Miskioglu, S. Gowtham and G. M. Odegard, *Carbon* **95** (2015) 100.
13. A. Catangiu, D. N. Ungureanu and V. Despa, *Mater. Mech.* **15**(12) (2017) 11.
14. J. M. Hodgkinson, *Mechanical Testing of Advanced Fibre Composites* (Woodhead Publishing, 2000).
15. F. Heieck, C. Kuon, A. Miene, P. Middendorf and A. S. Herrmann, *Compos. Struct.* **322** (2023) 117409.
16. E. Markiewicz, P. Ducrocq and P. Drazetic, *Int. J. Impact Eng.* **21**(6) (1998) 433.
17. M. Geers, R. De Borst and T. Peijs, *Compos. Sci. Technol.* **59**(10) (1999) 1569.
18. T. Kroupa, V. Laš and R. Zemčík, *J. Compos. Mater.* **45**(9) (2011) 1045.
19. P. Ragauskas and R. Belevičius, *Aviation* **13**(4) (2009) 109.
20. C. M. Soares, M. M. De Freitas, A. Araújo and P. Pedersen, *Compos. Struct.* **25**(1–4) (1993) 277.
21. A. L. Araújo, C. M. Soares and M. M. De Freitas, *Compos. B Eng.* **27**(2) (1996) 185.
22. A. Araújo, H. Lopes, M. Vaz, C. M. Soares, J. Herskovits and P. Pedersen, *Comput. Struct.* **84**(22–23) (2006) 1471.
23. F. Tao, X. Liu, H. Du and W. Yu, *Compos. Struct.* **272** (2021) 114137.
24. X. Liu, F. Tao and W. Yu, *Compos. Struct.* **252** (2020) 112658.
25. S. Sivanandam, S. Deepa, S. Sivanandam and S. Deepa, *Genetic Algorithms* (Springer, 2008).
26. A. Lambora, K. Gupta and K. Chopra, Genetic algorithm-a literature review, in *Int. Conf. Machine Learning, Big Data, Cloud and Parallel Computing (COMITCon)* (IEEE, 2019), pp. 380–384.
27. E. Comellas, S. I. Valdez, S. Oller and S. Botello, *Compos. Struct.* **122** (2015) 417.
28. A. I. Forrester and A. J. Keane, *Progress Aerospace Sci.* **45**(1–3) (2009) 50.
29. R. Rikards, H. Abramovich, J. Auzins, A. Korjakins, O. Ozolinsh, K. Kalnins and T. Green, *Compos. Struct.* **63**(2) (2004) 243.
30. E. Barkanov, E. Skukis and B. Petitjean, *J. Sound Vib.* **327**(3–5) (2009) 402.
31. J. Steuben, J. Michopoulos, A. Iliopoulos and C. Turner, *Compos. Struct.* **132** (2015) 694.
32. B. C. Csáji et al., *Hungary* **24**(48) (2001) 7.
33. K. Xu, D. Z. Huang and E. Darve, *J. Comput. Phys.* **428** (2021) 110072.
34. X. Liu, J. Qin, K. Zhao, C. A. Featherston, D. Kennedy, Y. Jing and G. Yang, *Compos. Struct.* **305** (2023) 116500.
35. L. Cappelli, G. Balokas, M. Montemurro, F. Dau and L. Guillaumat, *Compos. B Eng.* **176** (2019) 107193.
36. H. Mallikarachchi, Ph.D. thesis, University of Cambridge (2011).